Journal of the Korean Association for Shell and Spatial Structures
Vol. 6, No. 1 (통권 19호), pp. 45~54, March, 2006

더블앵글 접합부를 사용한 철골조의 단순해석 모델

Simplified Analytical Model for a Steel Frame with Double Angle Connections

양 재 근* 이 길 영** 박 정 숙**
Yang, Jae-Guen Lee, Gil-Young Park, Jeong-Suk

Abstract

A steel frame is one of the most commonly used structural systems due to its resistance to various types of applied loads. Many studies have been conducted to investigate the effects of connection flexibility, support conditions, and beam-to-column stiffness ratio on the story drift of a frame. Based on the results of these studies, several design guides have been proposed.

This research has been conducted to predict the actual behavior of a double angle connection, and to establish its effect on the story drift and the maximum allowable load of a steel frame. For these purposes, several experimental tests were conducted and a simplified analytical model was proposed. This simplified analytical model consists of four spring elements as well as a column member. In addition, a point bracing system was proposed to control the excessive story drift of an unbraced steel frame.

Keywords : double angle connection, unbraced frame, story drift, point-braced frame

1. Introduction

A double angle connection has been considered as an adequate connection type for low-rise steel frames due to its easiness and low cost of construction. The moment resistance capacity of a double angle connection depends on several parameters such as angle thickness, bolt gage distance, and number of bolts[3),5),6)]. Even though the double angle connection composed of relatively thick angles with short bolt gage distances can transfer significant moments to the supporting members, it has been designed as a simple shear connection. Therefore, it is necessary to predict the actual moment resistance capacity of a double angle connection, and to provide some basic data for the design of a steel frame with double angle connections. A steel frame with double angle connections can be designed optimally only when these requirements are fulfilled. The angle thickness and bolt gage distance of a double connection are selected as two main variables in performing experimental tests. A simplified analytical model is proposed to predict the actual behavior of a steel frame with double angle connections. This model consists of four spring elements and a column member. A rotational spring element attached to the top of the column member idealizes the double angle connection and its rotational spring stiffness can be obtained by experimental tests. By using this simplified analytical model, the story drift of a steel frame can be easily calculated. In addition, the maximum allowable loads without violating the story drift limit and reference moment limit can also be obtained.

* School of Architecture, Inha University, Incheon, Korea
Tel : 032-860-7588 Fax : 032-866-4624
E-mail : jyang@inha.ac.kr
** Graduate School Student of Architecture, Inha University, Incheon, Korea

2. Experimental Tests

Four experimental tests were conducted to obtain the actual moment-rotation curves of double angle connections. The rotational connection stiffness obtained from each curve can be substituted for the rotational stiffness of a spring element connected to the top of the simplified analytical model. L125×75×7 and L125×75×10 angle sections were considered. The geometry of an angle section is depicted in <Fig. 1> g1 is defined as the distance between the centerline of each bolt and the corner of an angle section. Each angle specimen had two different bolt gage distances such as g1=65mm, 90mm, respectively. The outstanding leg of each angle was connected to a H400×200×8×13(equivalent to W18×35) column with four F10T M20 bolts, while the back-to-back angle leg was welded to a H350 ×350×12×19(equivalent to W14×90) beam with 0.6cm E70xx fillet welds. Each bolt was tightened with 539 N·m corresponding to 147 kN, which is the bolt axial tensile load. Material properties of the angle specimen used in the tests were obtained from the coupon tests. The average values of the coupon tests are presented in <Table 1>.

The test set-up is shown in <Fig. 2>. The shear load was gradually applied to the tip of a beam, which stood vertically on a horizontally laid column, by an actuator at a speed of 1.5mm/min. A special device was introduced at both sides of the cantilever beam to prevent lateral buckling, which may occur in the beam. The rotation of the double angle connection was measured by using two pairs of LVDTs as shown in <Fig. 2>. The forces applied to the cantilever were recorded through the load cell in the actuator.

It is necessary to check the bolt strength and weld strength of a double angle connection subjected to the combined tensile and shear loads. In addition to the maximum allowable load that a bolt group can resist, the nominal tensile strength R_t and shear strength R_v of each bolt can be calculated as listed in <Table 2> by using the following equation (1) to equation (5)[1),9)].

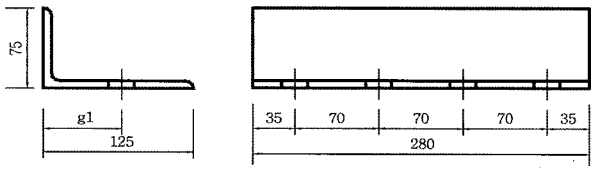

〈Fig. 1〉 Geometry of an angle considered in the analysis and test

〈Table 1〉 Material properties of the angle specimen and bolt

Test specimen	Young's modulus (N/mm^2)	Yield stress (N/mm^2)	Ultimate stress (N/mm^2)
angle	2.03×105	3.19×102	4.69×102
bolt	2.61×105	8.72×102	9.25×102

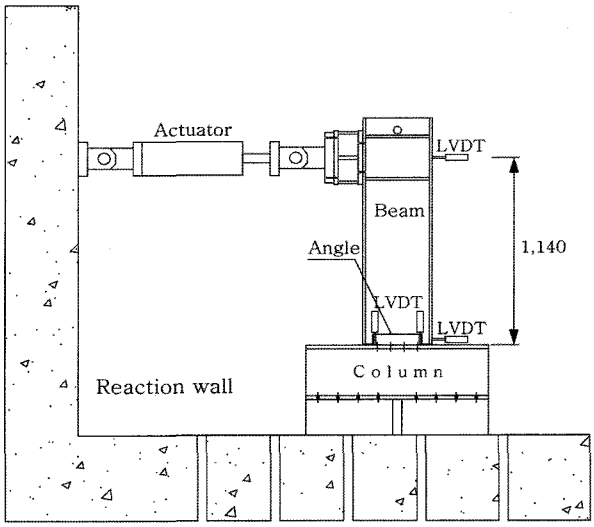

〈Fig. 2〉 Test set-up

〈Table 2〉 Nominal tensile and shear strength of each bolt used in experimental tests

e_1(mm)	y(mm)	Σy^2(mm^2)	Σn	F_v(N/mm^2)	T_b(N)	P(N)	R_t(N)	R_v(N)
1,140	105	49,000	8	117	142,000	40,800	98,000	5,000

$$R_t = A_b\left(\frac{M\,y}{\sum A_b\,y^2}\right) \quad (1)$$

$$\max R_v = F'_V\,A_b = R_v \quad (2)$$

where,

$$M = P e_1 \quad (3)$$

$$F'_V = F_V\left(1 - \frac{T}{0.8\,T_b\,N_b}\right) \quad (4)$$

$$R_v = \frac{P}{\sum n} \quad (5)$$

e_1 : distance from an applied load to the surface of a column flange

P : load applied to the tip of a beam

y : distance from the center of a bolt group to the outermost fastener

A_b : nominal unthreaded body area of a bolt

$\Sigma A_b\,y^2$: moment of inertia of the bolt areas

Σn : total number of bolts

F_v : maximum nominal service load shear stress of a bolt

T : nominal applied service load force

T_b : initial bolt tension force

N_b : number of bolts carrying nominal applied service load force

The maximum weld strength and the maximum allowable load that a weld group can resist can be calculated by an elastic method which uses the following equation (6) to equation (10) as listed in <Table 3>.

$$r_u = \sqrt{(r_{px} + r_{mx})^2 + (r_{py} + r_{my})^2}$$
$$\le \phi r_n = 0.75(0.6F_{E70} \times 0.707a) \quad (6)$$

where,

$$r_{px} = 0 \quad (7)$$

$$r_{py} = \frac{P}{l} \quad (8)$$

$$r_{mx} = \frac{P e_2 c_y}{I_p} \quad (9)$$

$$r_{my} = \frac{P e_2 c_x}{I_p} \quad (10)$$

l : total weld lengthe

e_2 : distance from an applied load to the center of a weld group

c_x : distance from the center of a weld group to the remote point in x-direction

c_y : distance from the center of a weld group to the remote point in y-direction

I_p : polar moment of inertial of a weld group

α : normal throat size

ϕ : resistance factor

In the experimental tests, the applied load should be less than the maximum load, P, respectively, listed in <Table 2> and <Table 3> to guarantee the safety of the double angle connection.

As the applied load increases, the upper corner of each angle specimen starts to move toward the symmetric plane of double angle connections. The stress concentrates on the edge of the bolt head and

〈Table 3〉 Weld strength of a double angle connection under the combined tensile and shear loads

Angle specime	e_2 (mm)	l (mm)	c_x (mm)	c_y (mm)	I_p (mm^3)	r_{px} (N)	r_{py} (N)	r_{mx} (N)	r_{my} (N)	r_u (N)	P (N)
L-7-90 L-7-65	1,076	406	52.1	140	4,986,368	0	108.0 (2.5P)	1.29 (30.0P)	473.0 (11.0P)	1,419 (33.0P)	43,000
L-10-90 L-10-65	1,076	406	52.2	140	5,051,247	0	119 (2.5P)	1,431 (30.0P)	525 (11.0P)	1,574 (33.0P)	47,700

the part in which the back-to-back angle leg and fillet meet. Stress concentration at the upper line of the fillet of each angle specimen finally leads to the failure of each angle specimen. Considering this failure mode, the excessive reduction of bolt gage distance and the further increase of angle thickness may cause an earlier failure of each angle specimen due to stress concentrations. <Fig. 3> represents the deformed shape of an L-7-65 angle specimen.

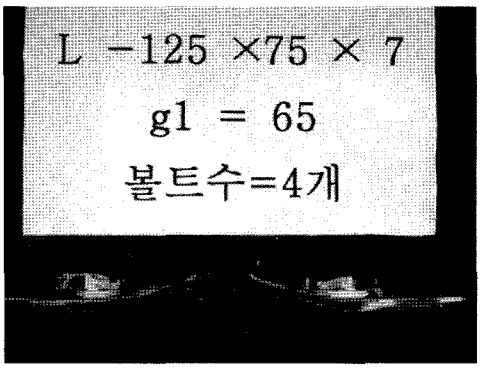

〈Fig. 3〉 Deformed shape of an L-7-65 angle specimen

Several analytical models, proposed by Richard, Frye-Morris, and Ang-Morris, have been commonly used to estimate the actual moment-rotation relationship of a double angle connection[2),7)].

The main parameters, such as initial rotational stiffness, plastic rotational stiffness, reference moment, and curve sharpness parameter as shown in <Fig. 4>, are introduced in the analytical model proposed by Richard[8)]. The curve sharpness parameter controls the rate of decay of the curve's slope within the given loading conditions. It is also important because it represents physically a measure of imperfections in the connections. On the other hand, the curve-fitting constants and the standardization constant are used in analytical models proposed by Frye-Morris and Ang-Morris. Each prediction equation can be written as follows:

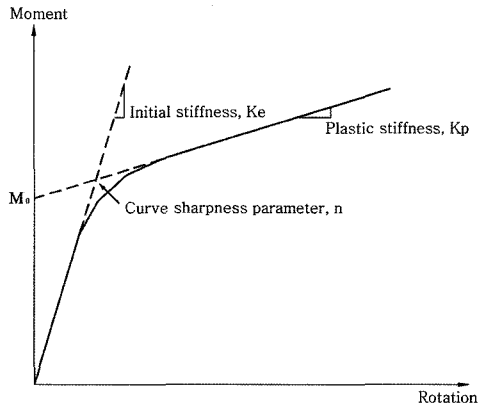

〈Fig. 4〉 Main parameters of Richard mode

Richard model-

$$M(\theta)=\frac{(K_e-K_p)\theta}{(1+\left|\frac{(K_e-K_p)\theta}{M_0}\right|^n)^{1/n}}+K_p\theta \tag{11}$$

where,

W : moment

θ : rotational angle

K_e : initial stiffness

K_p : plastic stiffness

M_0 : reference moment

n : curve sharpness parameter

Frye-Morris polynomial model-

$$\theta=C_1(KM)^1+C_2(KM)^3+C_3(KM)^5 \tag{12}$$

where,

$$K=d_a^{-2.4}\,t_a^{-1.81}\,g^{0.15} \tag{13}$$

$$C_1=3.66\times10^{-4} \tag{14}$$

$$C_2=1.15\times10^{-6} \tag{15}$$

$$C_3=4.57\times10^{-8} \tag{16}$$

C_1, C_2, C_3 : curve fitting constants

d_a : angle length

t_a : angle thickness

g : angle gage distance

Ang-Morris power model-

$$\frac{\theta}{(\theta_r)_0} = \frac{KM}{(KM)_0}\left[1+\left(\frac{KM}{(KM)_0}\right)^{n-1}\right] \quad (17)$$

where,

$$K = d_a^{-2.2}\, t_a^{0.08}\, g^{-0.28} \quad (18)$$

$$(\theta_r)_0 = 3.98\times10^{-3} \quad (19)$$

$$(KM)_0 = 0.63 \quad (20)$$

$$n = 4.94 \quad (21)$$

As depicted in <Fig. 5>, each moment-rotation curve shows almost a linear relationship until its angular change reaches to 0.005(rad.) and flattens out rapidly as the moment increases. Main parameters that describe the actual behavior of each double angle connection are listed in <Table 4>.

The initial rotational stiffness and plastic stiffness obtained from each experimental test are smaller than those simulated by Frye-Morris polynomial model and Ang-Morris power model. The thicker

〈Table 4〉 Main parameters for each double angle connection

Specimen		K_e (N-mm/rad)	K_p (N-mm/rad)	M_0 (N-mm)	n
L-7-90	Test	4,571.8	246.6	14.8	1.3
	F-M	7,319.3	518.6	22.6	1.8
	A-M	7,097.3	580.8	24.7	2.1
L-7-65	Test	4,841.2	333.2	19.9	1.6
	F-M	7,691.1	576.8	24.1	1.7
	A-M	6,546.9	490.1	23.3	2.0
L-10-90	Test	4,870.6	411.6	24.5	1.4
	F-M	13,973.2	978.1	43.3	1.8
	A-M	6,856.2	620.4	23.2	2.2
L-10-65	Test	6,232.8	686	33.8	1.8
	F-M	14,595.2	1,063.3	44.8	1.8
	A-M	6,315.0	530.6	21.8	2.1

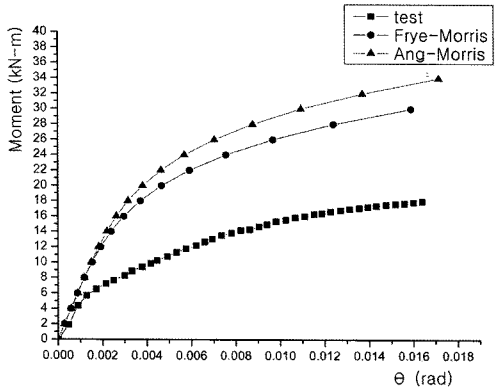

(a) L-7-90

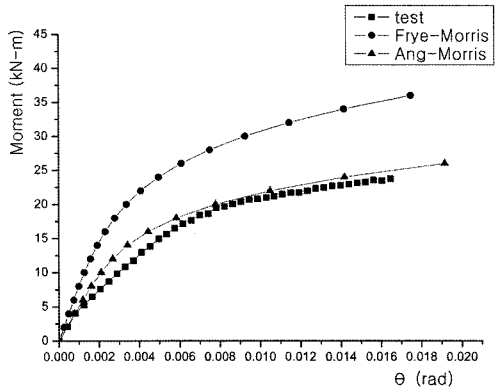

(b) L-7-65

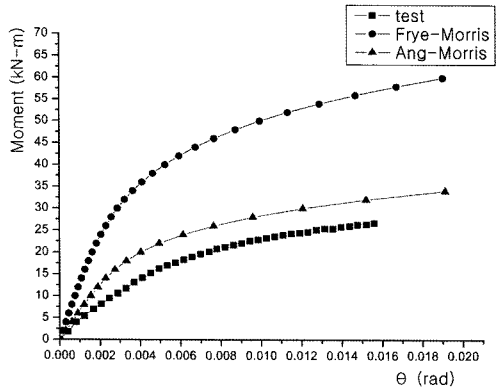

(c) L-10-90

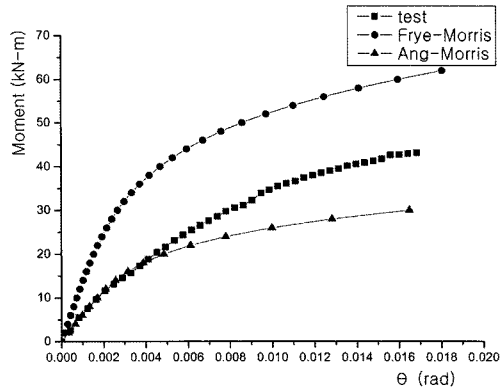

(d) L-10-65

〈Fig. 5〉 Moment-rotation curves of each double angle connection

the angle and the shorter the bolt gage distance, the larger the initial rotational stiffness obtained. However, it is much more effective way to increase the rotational stiffness by reducing the bolt gage distance than by increasing the angle thickness as shown in Table 4. When g1=90mm, the initial rotational stiffness increases about 6.5% as the angle thickness increase from t=7mm to t=10mm. On the other hand, the initial rotational stiffness increases about 5.9% as the bolt gage distance decrease from g1=90mm to g1=65mm.

3. Simplified Analytical Model

Many studies have been conducted to predict the effects of beam-to-column stiffness ratio, loading and support conditions, and rotational connection stiffness on the actual behavior of a steel frame. Unfortunately, very limited information is available on the behavior of a low-rise frame with double angle connections.

Thus, a simplified analytical model as shown in <Fig. 6> is suggested to provide some information on the effects of connection flexibility and support conditions on the story drift and maximum allowable loads of a steel frame with double angle connection.

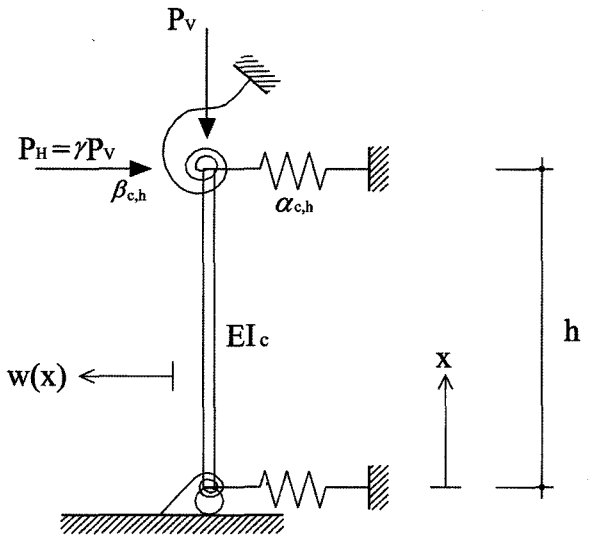

〈Fig. 6〉 Simplified analytical model

This simplified model consists of four spring elements as well as a column member. Two spring elements attached to the top of the column member represent the actual behavior of double angle connections, while the other two spring elements attached to the bottom of the column member represent the support conditions of a steel frame. The moment inertia of the column member used in the simplified analytical model Ic is the sum of the moment inertia of the column member used in the actual steel frame. The vertical load applied to the simplified model P_V is the summation of the vertical loads applied at the top of the column member used in the steel frame.

The story drift of a steel frame can be obtained by using the simplified analytical model as follows:

$$w(x)=\left[\frac{6\{2(\beta_0+\beta_h)-hk_V^{\,2}(2+\beta_h)+2\beta_0\beta_h h\}k_H^{\,2}}{D}\right] +\left[\frac{6\alpha_0 h(2+\beta_h h)k_H^{\,2}}{D}\right]x +\left[\frac{3\alpha_0\beta_0 h(2+\beta_h h)k_H^{\,2}}{D}\right]x^2 +\left[\frac{-2\alpha_0(\beta_0+\beta_0\beta_h+\beta_h)k_H^{\,2}}{D}\right]x^3 \quad (22)$$

where,

$$\alpha_0=\frac{\alpha_{C,0}}{EI_C},\quad \beta_0=\frac{\beta_{C,0}}{EI_C},\quad \alpha_h=\frac{\alpha_{C,h}}{EI_C},\quad \beta_h=\frac{\beta_{C,h}}{EI_C} \quad (23)$$

$$k_V=\sqrt{\frac{P_V}{EI_C}},\quad k_H=\sqrt{\frac{P_H}{EI_C}} \quad (24)$$

$$D=6hk_V^{\,2}\{h(\alpha_0\beta_0+\alpha_h\beta_h)+2(\alpha_0+\alpha_h)\} -4\alpha_0\alpha_h h^2\{h(\beta_0+\beta_h)+3\} -12(\alpha_0+\alpha_h)(\beta_0+\beta_h) -12\beta_0\beta_h h(\alpha_0+\alpha_h)-\alpha_0\alpha_h\beta_0\beta_h h^4 \quad (25)$$

I_c : moment of inertia of a column used in the simplified model

$I_{f,c}$: moment of inertia of a column used in the

steel frame

N : total number of columns used in the frame

Application feasibility of the story drift of an unbraced frame is verified by using this analytical model. The unbraced frame has fixed base supports and it can have either pinned connections or rigid connections as shown in <Fig. 7>. A horizontal load is only applied to the upper left corner of the steel frame in this case. For a steel frame with pinned connections, the spring stiffnesses of the simplified model can be assumed as $\alpha_0 = \infty$, $\beta_0 = \infty$, $\alpha_h = 0$, and $\beta_h = 0$. By substituting these values into equation (22), the coefficients and story drift of the frame can be calculated as follows:

$$A_1 = A_2 = 0, \quad A_3 = -\frac{P_H h}{2EI_C}, \quad A_4 = \frac{P_H}{6EI_C} \tag{26}$$

$$w(x) = -\frac{P_H h^3}{6EI_{f,C}} \tag{27}$$

On the other hand, the spring stiffnesses of the simplified model can be assumed as $\alpha_0 = \infty$, $\beta_0 = \infty$, $\alpha_h = 0$, and $\beta_h = \infty$ for a steel frame with rigid connections. By substituting these values into equation (22), the coefficients and story drift of the frame can be obtained as follows:

$$A_1 = A_2 = 0, \quad A_1 = A_2 = 0, \quad A_4 = \frac{P_H}{6EI_C} \tag{28}$$

$$w(x) = -\frac{P_H h^3 (2LI_{f,C} + 3I_b h)}{12EI_{f,C}(LI_{f,C} + 6I_b h)} \tag{29}$$

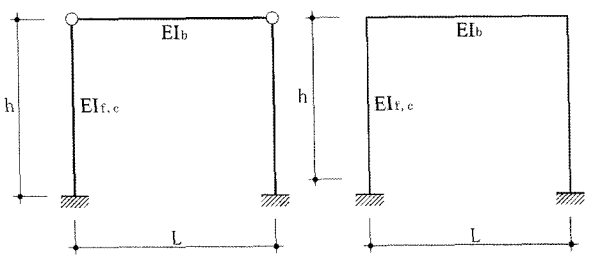

(a) Pinned connections (b) Rigid connections

〈Fig. 7〉 A steel frame with fixed base supports

The story drifts of this unbraced frame considered show exactly the same values as those obtained from the previous studies[4]. Thus, this simplified model can be utilized to establish the actual behavior of a steel frame with double angle connections under various loadings and support conditions.

Allowed to move horizontally ($\alpha_h = 0$), a frame connected by double angles with fixed base supports ($\alpha_0 = \infty$, $\beta_0 = \infty$) has been considered to calculate the story drift and maximum allowable loads. The rotational spring stiffnesses obtained from the results of the experimental tests are β_h=0.056(L-7-90), 0.060 (L-7-65), 0.060(L-10-90), and 0.077(L-10-65), respectively. By substituting these connection stiffnesses into equation (22), the story drifts of the frame with double angles can be written as follows:

$$w(h) = \frac{h^3 P_H (500 + 7h)}{12(-250EI_{f,C} - 14hEI_{f,C} + 125h^2 P_{V,f})}$$

(L-7-90) (30)

$$w(h) = \frac{h^3 P_H (200 + 3h)}{24(-50EI_{f,C} - 3hEI_{f,C} + 25h^2 P_{V,f})}$$

(L-7-65), (L-10-90) (31)

$$w(h) = \frac{h^3 P_H (4{,}000 + 77h)}{24(-1{,}000EI_{f,C} - 77hEI_{f,C} + 500h^2 P_{V,f})}$$

(L-10-65) (32)

The story drifts of the steel frame with lower rotational connection stiffness are greater than those of the frame with higher rotational connection stiffness when the same horizontal and vertical loads are applied to the frame. The excessive story drift may destabilize a steel frame under horizontal and vertical loads. To stabilize a steel frame, the steel frame should satisfy the wind-drift limit($w(h) \leq h/400$) under a 50-year wind. <Table 5> represents the maximum allowable horizontal and vertical loads for a steel frame with dimensions h=3.5m and L=6m, and $i = I_b/I_{f,c}$=0.588. The wind-drift limit of this frame is satisfied only when the applied

$$M(h)=\frac{7h^2 EI_{f,C}\gamma P_{V,f}}{2(-250EI_{f,C}-14hEI_{f,C}+125h^2 P_{V,f})} \quad \text{(L-7-90)} \quad (33)$$

$$M(h)=\frac{3h^2 EI_{f,C}\gamma P_{V,f}}{4(-50EI_{f,C}-3hEI_{f,C}+25h^2 P_{V,f})} \quad \text{(L-7-65), (L-10-90)} \quad (34)$$

$$M(h)=\frac{77h^2 EI_{f,C}\gamma P_{V,f}}{4(-1000EI_{f,C}-77hEI_{f,C}+500h^2 P_{V,f})} \quad \text{(L-10-65)} \quad (35)$$

$$w(h)=-\frac{h^3\gamma P_{V,f}(500+7h)}{(3{,}000EI_{f,C}-1{,}500h^2P_{V,f}+500h^3K+168hEI_{f,C}+7h^4K)} \quad \text{(L-7-90)} \quad (36)$$

$$w(h)=-\frac{h^3\gamma P_{V,f}(200+3h)}{(1{,}200EI_{f,C}-600h^2P_{V,f}+200h^3K+72hEI_{f,C}+3h^4K)} \quad \text{(L-7-65), (L-10-90)} \quad (37)$$

$$w(h)=-\frac{h^3\gamma P_{V,f}(400+77h)}{(24{,}000EI_{f,C}-12{,}000h^2P_{V,f}+4{,}000h^3K+1{,}848hEI_{f,C}+77h^4K)} \quad \text{(L-10-65)} \quad (38)$$

$$K=\frac{1}{h^3(500+7h)}\left[h^2P_{V,f}\{400\gamma(500+7h)+1{,}500\}-EI_{f,C}(3{,}000+168h)\right] \quad \text{(L-7-90)} \quad (39)$$

$$K=\frac{1}{h^3(200+3h)}\left[h^2P_{V,f}\{400\gamma(200+3h)+600\}-EI_{f,C}(1{,}200+72h)\right] \quad \text{(L-7-65), (L-10-90)} \quad (40)$$

$$K=\frac{1}{h^3(4{,}000+77h)}\left[h^2P_{V,f}\{400\gamma(4{,}000+77h)+12{,}000\}-EI_{f,C}(24{,}000+1{,}848h)\right] \quad \text{(L-10-65)} \quad (41)$$

horizontal and vertical loads are less than the maximum allowable loads listed in <Table 5>.

From the regression analysis of the moment-rotation curves obtained from experimental tests, the reference moments are M_0=14.8kN(L-7-90), 19.9kN (L-7-65), 24.5kN(L-10-90), and 33.8kN(L-10-65), respectively. Since the slope of each moment-rotation curve decreases rapidly around the reference moment of each double angle connection, the connection moment M(h) should be less than or equal to its reference moment. The maximum allowable horizontal and vertical loads can be obtained from the following equation (33) to equation (35). Table 6 represents the maximum allowable horizontal and vertical loads that satisfy each connection moment limit ($M(h) \leq M_0$).

By comparing the maximum allowable horizontal and vertical loads listed in <Table 5> and <Table 6>, the story-drift of a steel frame can be the governing limit state except in the case of L-7-90. When the combined horizontal and vertical loads, which are greater than the maximum allowable loads listed in <Table 5> and <Table 6>, are applied to the steel frame, the frame should be braced to

〈Table 5〉 Maximum allowable horizontal and vertical loads satisfying the wind-drift limit unit : (N)

angle	β_h	r			
		0.5	1.0	1.5	2.0
		$P_{v,f}$	$P_{v,f}$	$P_{v,f}$	$P_{v,f}$
L-7-90	0.056	221,820	111,700	74,640	56,050
L-7-65	0.060	223,680	112,630	75,260	56,520
L-10-90	0.060	223,680	112,630	75,260	56,520
L-10-65	0.077	231,450	116,530	77,870	58,470

〈Table 6〉 Maximum allowable horizontal and vertical loads satisfying the reference moment limit unit : (N)

angle	β_h	r			
		0.5	1.0	1.5	2.0
		$P_{v,f}$	$P_{v,f}$	$P_{v,f}$	$P_{v,f}$
L-7-90	0.056	203,750	102,540	68,510	51,440
L-7-65	0.060	257,840	129,970	86,880	65,250
L-10-90	0.060	316,260	159,710	106,830	80,260
L-10-65	0.077	356,160	180,000	120,430	90,490

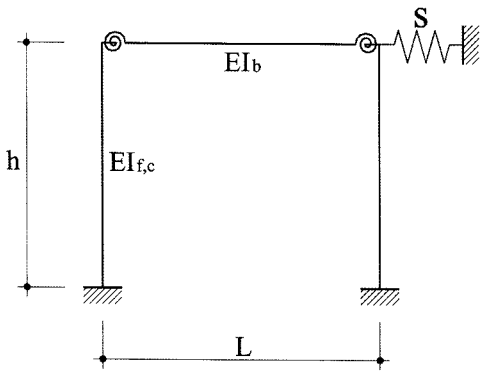

〈Fig. 8〉 A point-braced frame with double angle connections

prevent its instability due to excessive story drifts.

A point bracing system is introduced to control the excessive story drifts of a steel frame as shown in <Fig. 8>. The translational spring element acts independently with the stiffness of $S = K/EI_c$. The behavior of this braced frame with double angle connections can also be predicted by using the simplified analytical model. The braced frame has fixed base supports, and its horizontal movement can be restrained by the spring element attached to the upper right corner of the steel frame($\alpha_0 = \infty$, $\beta_0 = \infty$, $\alpha_h = S = K/EI_c$).

The rotational stiffness of each connection is the same as that of the unbraced frame considered. By substituting these connection stiffnesses into equation (22), the story drifts of the point- braced frame with fixed base supports can be written as follows:

The required translational spring stiffness of each point-braced frame can be obtained by using the above equations (36) to (38) and the wind drift limit ($w(h) \leq h/400$).

As shown in <Fig. 9>, the story drifts of the fixed base frame rapidly decrease as $K \rightarrow 10^3$N/mm when the maximum horizontal and vertical loads are applied to the point-braced frame. When $K \rightarrow 10^7$N/mm, the translational spring element acts as a pin support and no story drift can occur in the braced frame. The translational spring stiffness should be increased to satisfy the story drift limit

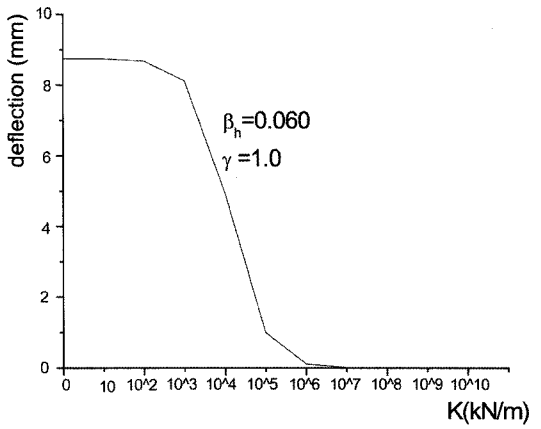

〈Fig. 9〉 Story drifts of the braced frame with fixed base supports when $P_{applied} = P_{max}$

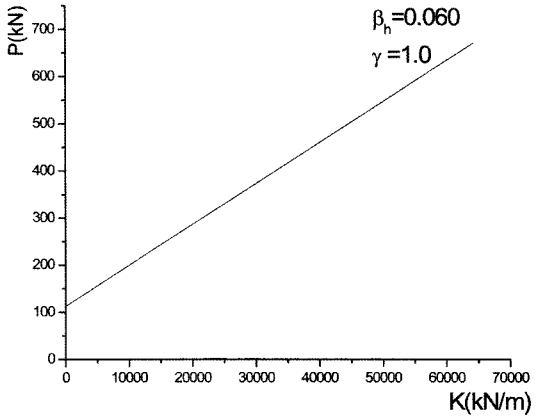

〈Fig. 10〉 The applied load-translational spring stiffness relationship of the braced frame with fixed base supports when $P_{applied} > P_{max}$

when the applied loads are greater than the maximum allowable loads listed in <Table 5> and <Table 6>, <Fig. 10> represents the applied load-translational spring stiffness relationship of the braced frame with fixed base supports when the applied loads are greater than the maximum allowable loads.

4. Conclusions

A frame with double angle connections has been studied to investigate the effects of the connection flexibility on its story drift control. Several experimental tests were conducted to obtain rotational stiffnesses

of double angle connections. The rotational stiffnesses of double angle connections considered are mainly influenced by the angle thicknesses and bolt gage distances in this research. A simplified model composed of spring elements is suggested to calculate the story drifts and maximum allowable loads that a steel frame can resist. These spring elements simulate the actual behavior of double angle connections and support conditions. A point-braced frame is also suggested to control the excessive story drifts of an unbraced frame in this research. The following conclusions are made from this research.

1. The thicker the angle and the shorter the bolt gage distance, the larger the initial rotational stiffness obtained. However, an earlier failure due to stress concentration may occur because of the excessive reduction of bolt gage distance and increase of angle thickness.
2. The higher the connection stiffness, the lower the story drift of the frame considered. However, a bracing system should be provided for a steel frame with double angle connections since the rotational stiffnesses of double angle connections are rapidly decreased around their reference moments.
3. When the applied loads are greater than the maximum allowable loads listed in Tables 5 and 6, the translational spring stiffness of the point-braced frame has to be increased to satisfy the wind-drift limit, and it can be also calculated easily by using the suggested spring model.

References

1. AISC, Manual of Steel Construction *Load & Resistance Factor Design*, 3rd ed. Volumes 1 and 2. Chicago : AISC, 2001
2. Chen, W.F., *Joint flexibility in steel frames.* Elsevier Applied Science. 1998
3. De Stefano, M., Astaneh, A., Axial force-displacement behavior of steel double angles. *Journal of Construct Steel Research*, 20, 1991, pp.161~180
4. Galambos T.V. Editor., *Guide to stability design criteria for metal structures*, 5th ed. John Wiley & Sons, 1998
5. Hong K., Yang J.G., Lee S.K., Moment-rotation behavior of double angle connections subjected to shear load. *Journal of Structural Engineering*, 24, 2002, pp.125~132
6. Kishi, N., Chen, W.F., Moment-rotation relationship of semi rigid connection with angles. *Journal of Structural Engineering*, 116, 1990, pp.1813~1834
7. Lorenz, R.F., Kato, B., Chen, W.F. Editors., *Semi-rigid connections in steel frames.* CTBUH. McGraw-Hill, 1992
8. Richard, R.M., Hisa, W.K., Chmieelowiec M., Derived moment rotation curves for double framing angles. *Computers & Structures*, 30, 1988, pp.485~494
9. Salmon, C.G., Johnson, J.E., Steel *Structures: design and behavior*, 4th ed. Harper Collins, 1996